THE JOURNAL OF PHYSICAL CHEMISTRY C

Article

pubs.acs.org/JPCC

Activation and Stabilization of Nitrogen-Doped Carbon Nanotubes as Electrocatalysts in the Oxygen Reduction Reaction at Strongly Alkaline Conditions

Anqi Zhao,[†] Justus Masa,[‡] Wolfgang Schuhmann,[‡] and Wei Xia*[,†]

[†]Laboratory of Industrial Chemistry and [‡]Analytische Chemie—Elektroanalytik & Sensorik, Ruhr-University Bochum, 44801 Bochum, Germany

ABSTRACT: Nitrogen-doped carbon nanotubes (NCNTs) are highly active electrocatalysts in the oxygen reduction reaction (ORR) at alkaline conditions. However, the initial activation and stabilization of NCNTs have rarely been investigated at industrially relevant conditions. Three types of NCNTs were synthesized by catalytic growth (NCNT-growth) or posttreatment of oxygen-functionalized CNTs with NH_3 (NCNT-NH_3) or aniline (NCNT-aniline). The obtained NCNTs were treated in 10 M KOH at 80 °C for 5 h, and the formation of oxygen groups by alkaline treatment and their interaction with existing nitrogen groups was analyzed. X-ray photoelectron spectroscopy showed that the concentrations of pyridinic and quaternary nitrogen increased in NCNT-growth due to the KOH treatment accompanied by the decrease of pyrrolic nitrogen, whereas the nitrogen groups changed differently in NCNT-NH_3 and NCNT-aniline. NCNT-NH_3 showed the highest ORR activity before alkaline treatment. After the treatment, the activity of NCNT-growth was higher, whereas those of NCNT-NH_3 and NCNT-aniline were lower. These results were found to be correlated with changes in the nitrogen groups caused by alkaline treatment. Furthermore, NCNTs showed different C═O/C−O ratios after alkaline treatment as compared to a strong increase of C−O in CNTs, indicating that the presence of nitrogen in NCNTs influences the formation of oxygen groups on carbon and surface oxidation.

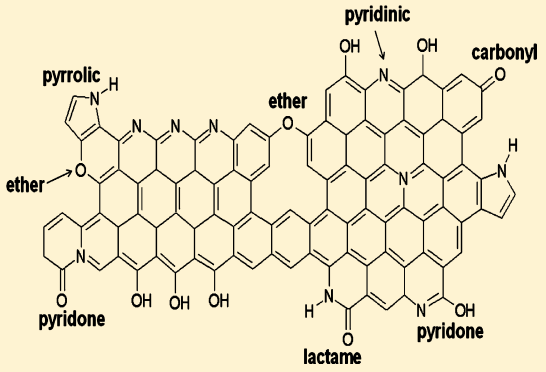

1. INTRODUCTION

The oxygen reduction reaction (ORR) under alkaline conditions is an important electrochemical process in alkaline fuel cells,[1,2] metal−air batteries,[3] and brine electrolysis.[4] The development of active, stable, and cost-effective electrocatalysts is a great challenge for these applications. Pt- and Rh-based catalysts have been used for ORR at acidic conditions, for which the major challenges are high cost, slow kinetics, and insufficient stability.[5,6] At alkaline conditions, Ag-based catalysts showed high catalytic activity and reasonable long-term stability.[7,8] For example, Ag supported on carbon black is used as an ORR catalyst in brine electrolysis in the chemical industry.[9] In zinc−air batteries, manganese oxide is commonly used as an electrocatalyst for ORR at alkaline conditions.[10]

Recently, transition metal N_4-macrocyclic complexes have attracted enormous interest as low-cost alternatives to noble-metal catalysts for ORR.[11,12] In the past few years, N-doped carbon materials in the absence and presence of metals have been intensively studied as noble metal-free catalysts for ORR at alkaline conditions.[13−18] In particular, nitrogen-doped carbon nanotubes (NCNTs) are a major focus due to their unique physical and chemical properties including high conductivity and chemical resistance.[19,20] Furthermore, the ORR performance can be improved through codoping of carbon materials by boron and nitrogen.[21,22]

Different types of nitrogen-containing groups can be incorporated in CNTs including pyridinic, pyrrolic, and quaternary-type nitrogen.[23,24] Nitrogen embedding in the surface of CNTs also leads to the formation of surface defects such as edge planes.[25,26] Earlier studies suggested that pyridinic nitrogen could improve ORR activity due to the conjugation effect of the nitrogen lone pair electrons and the graphene π system.[27,28] Recently, more evidence has been found that quaternary-type nitrogen also contributes to the enhanced ORR activity especially at alkaline conditions.[29,30] Theoretical studies support the hypothesis that the presence of quaternary-type nitrogen favors O_2 adsorption at carbon sites on the zigzag edges located adjacent to quaternary-type nitrogen.[31] In contrast, pyrrolic nitrogen has been suggested to have negative effects on the rate of the ORR.[32,33] Our previous results demonstrated that ORR activity is directly related not to the total nitrogen amount, but to the concentrations of pyridinic and quaternary nitrogen species.[34]

Although the various nitrogen groups contribute differently to ORR catalysis, controlled synthesis of certain groups remains a great challenge so far. Generally, NCNTs can be synthesized either by direct catalytic growth[35] or by posttreatment[10,36]

Received: June 16, 2013
Revised: September 19, 2013
Published: October 22, 2013

dx.doi.org/10.1021/jp4059438 | J. Phys. Chem. C 2013, 117, 24283−24291

using nitrogen-containing precursors. In the case of direct growth, nitrogen species are present on the surface and in the bulk of the obtained NCNTs. In contrast, nitrogen species are usually formed exclusively on the surface or in the near-surface layers of the NCNTs synthesized when applying the posttreatment method. While the ORR activity is not directly related to the total amount of nitrogen incorporated in CNTs,[34] the location and nature of the nitrogen species can possibly influence the electrochemical stability of NCNTs.

As a typical three-phase reaction, the ORR proceeds only when sufficient contact among these phases can be achieved. For the efficient release of the produced H_2O in the ORR, the electrode has to be hydrophobic. Otherwise, the electrode can be flooded due to H_2O accumulation, and the diffusion of molecular oxygen will be impeded or even blocked leading to an increase of overpotential or to cell failure. On the other hand, nitrogen doping of CNTs often leads to the decrease of hydrophobicity. One of the reasons is that nitrogen doping often involves preoxidation, for example, by HNO_3.[26] Even for directly grown NCNTs without preoxidation, oxygen and nitrogen groups as well as surface defects always coexist on NCNTs, which decrease the hydrophobicity and are unfavorable for the ORR. Additionally, the electrocatalytic ORR itself in concentrated alkaline electrolyte can change the surface wettability of NCNT electrode and shorten its lifetime.

While the interest in N-doped carbon materials as electrocatalysts continues to grow, the electrochemical stability and the wetting properties of these catalysts have rarely been studied. Particularly, the ORR under industrially relevant conditions, for example, in 10 M KOH and at 80 °C typically used in the chlor-alkali industry, has seldom been investigated. Here, we report on the stability of three different types of NCNTs synthesized either by direct growth or by posttreatment using different precursors. The obtained NCNTs were treated in 10 M KOH at 80 °C for 5 h. The NCNT samples before and after the alkaline treatment were characterized and tested as electrocatalysts for the ORR in 0.1 or 1.0 M KOH. The focus of this study is not the long-term stability from an industrial point of view, but the initial activation and stabilization stage.

2. EXPERIMENTAL SECTION

2.1. Sample Preparation and Alkaline Treatment. Three types of nitrogen-doped CNTs were prepared and investigated. (1) Catalytically grown NCNTs (outer diameter 13−16 nm, Bayer AG, Leverkusen, Germany) were purified by washing in 1.5 M HNO_3 under stirring for 72 h at room temperature to remove the residual metal catalysts used in their synthesis. The obtained NCNTs were denoted as NCNT-growth. (2) NCNTs were obtained by the posttreatment of regular CNTs with NH_3 (inner diameter 2−6 nm, outer diameter 13−16 nm, BET surface area 280 $m^2\ g^{-1}$, Bayer AG, Leverkusen, Germany). In a typical synthesis, as-received CNTs were first washed in 1.5 M HNO_3 under stirring for 72 h at room temperature. The washed CNTs were then functionalized via HNO_3 vapor treatment at 200 °C for 72 h to introduce oxygen-containing functional groups.[37] The oxygen-functionalized CNTs were loaded into a tubular reactor with an inner diameter of 30 mm and treated at 600 °C for 6 h under flowing ammonia (10 vol % NH_3 in He) at a flow rate of 50 sccm. The obtained NCNTs were denoted as NCNT-NH_3. (3) Similarly, oxygen-functionalized CNTs were loaded into a tubular reactor, and after the temperature was raised to 800 °C under flowing helium, aniline vapor was introduced into the reactor for 2 h by passing helium (50 sccm) through a saturator filled with aniline (99%, Aldrich) at room temperature. The obtained NCNTs were denoted as NCNT-aniline.

The alkaline treatment of the NCNTs was performed at 80 °C in 10 M KOH for 5 h under stirring. Typically, 15 mg of NCNTs was added to 15 mL of KOH solution (10 M) in a polypropylene vial, which was sealed in air and heated in an oil bath to 80 °C for the treatment. After cooling to room temperature, the samples were washed thoroughly using deionized water and dried at 60 °C overnight before further applications.

2.2. Characterization. X-ray photoelectron spectroscopy (XPS) measurements were carried out in an ultrahigh vacuum setup equipped with a monochromatic Al Kα X-ray source (1486.6 eV; anode operating at 14.5 kV and 45 mA) and a high resolution Gammadata-Scienta SES 2002 analyzer. The base pressure in the measurement chamber was maintained at about 7×10^{-10} mbar. The XP spectra were recorded in the fixed transmission mode with a pass energy of 200 eV. Charging effects were compensated by applying a flood gun. The binding energies were calibrated based on the graphite C 1s peak at 284.5 eV. The CASA XPS program with a Gaussian−Lorentzian mix function and Shirley background subtraction was used to analyze the XP spectra quantitatively. The peak positions for all the samples were reproducible using a fixed Gaussian to Lorentz ratio of 70:30 and fixed fwhm's.

Temperature-programmed oxidation (TPO) measurements were carried out in a horizontal quartz tube reactor with an inner diameter of 3 mm. An online infrared detector (Bühler Technologies, Germany) was used to determine quantitatively the release of CO and CO_2, which was calibrated in the range 0−4000 ppm by standard gas mixtures prior to the measurements. For each measurement, 5.0 mg of sample was heated from room temperature to 800 °C at a heating rate of 1 K min^{-1} under flowing O_2 (5 vol % O_2 in He) at a flow rate of 30 sccm.

2.3. Electrochemical ORR Tests. Electrochemical measurements were performed in a conventional three-electrode cell using glassy carbon (Ø 4 mm; HTW, Germany) modified with the NCNTs as the working electrode, a reversible hydrogen electrode (RHE) as the reference electrode, and a Pt foil as the counter electrode. Prior to experiments, the glassy carbon electrode was polished on a polishing cloth using different alumina pastes (3.0, 1.0, 0.3, and 0.05 μm) to obtain a mirrorlike surface followed by ultrasonic cleaning in water. For preparation of the working electrode, 5.0 mg of the catalyst were dispersed ultrasonically for 30 min in a mixture of water (490 μL), ethanol (490 μL) and Nafion (5%, 20 μL). 5.3 μL of the resulting catalyst suspension were dropped onto the polished glassy carbon electrode to obtain a catalyst loading of 210 $\mu g\ cm^{-2}$ (26.5 μg in total on the electrode). The electrode was dried in air at room temperature before the measurement.

Cyclic voltammetry (CV) and rotating disk electrode (RDE) measurements were carried out in 0.1 or 1.0 M KOH saturated with argon or oxygen at room temperature using an Autolab potentiostat/galvanostat (PGSTAT12, Eco Chemie, Utrecht, The Netherlands) in combination with a speed control unit (CTV101) and a rotating disk electrode rotator (EDI101; Radiometer, Villeurbanne, France). All experiments were carried out at room temperature in the potential range +1.0

dx.doi.org/10.1021/jp4059438 | J. Phys. Chem. C 2013, 117, 24283−24291

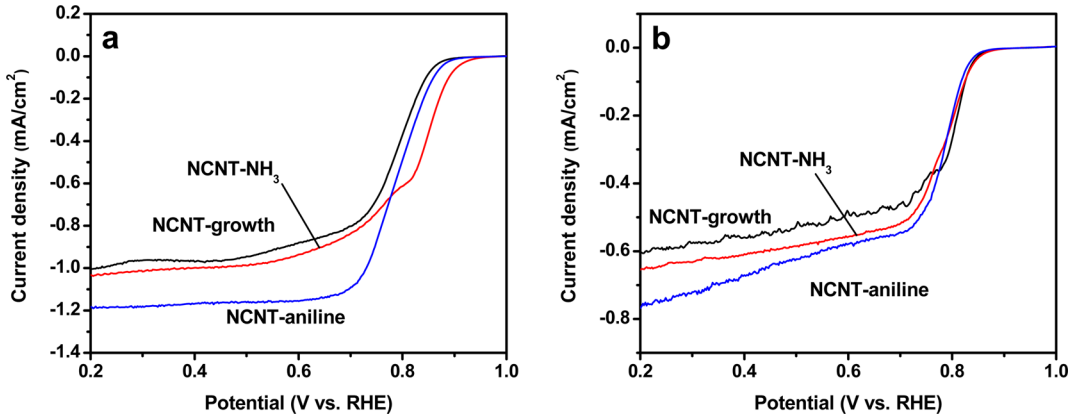

Figure 1. Linear sweep voltammograms of NCNTs synthesized by different methods. Measurements were performed at a scan rate of 5 mV s^{-1} and a rotation rate of 100 rpm in O_2-saturated electrolyte. (a) 0.1 M KOH; (b) 1.0 M KOH.

to 0.2 V at a scan rate of 5 mV s^{-1} after purging with argon or oxygen for 20 min.

3. RESULTS AND DISCUSSION

3.1. ORR Activity. The ORR catalytic activity of nitrogen-doped CNTs was studied by rotating disk electrode measurements in oxygen-saturated 0.1 and 1.0 M KOH at a scan rate of 5 mV s^{-1}. Before each measurement, the sample was evaluated in an Ar-saturated electrolyte and the obtained background voltammogram was subtracted from that measured in O_2-saturated electrolyte. Figure 1a shows the RDE results obtained in 0.1 M KOH. The oxygen reduction of the samples NCNT-NH_3 and NCNT-growth was under mixed kinetic/diffusion control between 0.97 and 0.67 V, whereas the NCNT-aniline sample showed a well-defined kinetic region. The onset potential of NCNT-NH_3 was more positive than for NCNT-growth and NCNT-aniline (Table 1). The slight distortion observed for sample NCNT-NH_3 is considered to be due to the activation of additional active sites that are not active at higher potentials.

Table 1. Onset Potential (E_{onset}) and Electron Transfer Number (n) in the ORR with Different NCNT Catalysts

	before alkaline treatment				after alkaline treatment[a]	
	0.1 M KOH		1.0 M KOH		0.1 M KOH	
sample	E_{onset}[b] (V)	n[c]	E_{onset} (V)	n	E_{onset} (V)	n
NCNT-growth	0.903	2.9	0.883	3.2	0.913	4.0
NCNT-NH_3	0.962	2.9	0.892	3.3	0.889	2.7
NCNT-aniline	0.914	3.4	0.879	3.8	0.889	2.5

[a]The alkaline treatment was performed in 10 M KOH at 80 °C for 5 h. [b]Determined when a current density of 0.01 mA cm^{-2} was reached. [c]Determined at 0.374 V in 0.1 and 1.0 M KOH electrolyte.

At a higher KOH concentration of 1.0 M all three NCNTs show similar ORR behavior (Figure 1b), although both the onset potential and reduction current were lower than in 0.1 M KOH. The onset potentials of NCNT-growth and NCNT-aniline were found to be decreased by about 20 and 35 mV, respectively. In contrast, a decrease of 70 mV was recorded for NCNT-NH_3 in 1.0 M KOH (Table 1). These results indicate that the ORR active sites of the NCNTs are sensitive to the pH of the electrolyte. Especially, the catalytic activity of NCNT-NH_3 was significantly lowered by the highly concentrated KOH.

Electrocatalysts are typically capable of continuous operation for years in the chlor-alkali industry. The initial activation and stabilization stage is critical for the long-term stability of the catalysts. Hence, we treated the three types of NCNT samples under industrially relevant conditions at 80 °C in 10 M KOH. After treatment for 5 h, the onset potential of NCNT-growth increased by 10 mV in 0.1 M KOH, whereas the onset potentials of NCNT-aniline and NCNT-NH_3 decreased by 25 and 73 mV, respectively (Figure 2). As a result, the onset

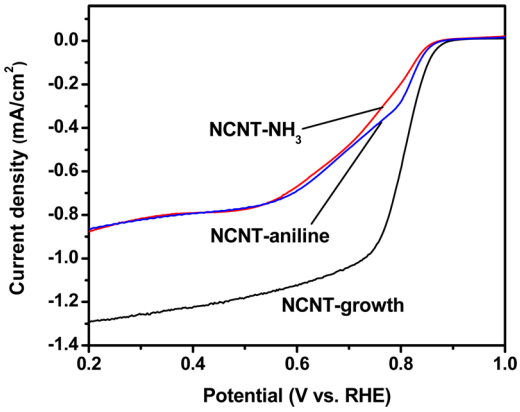

Figure 2. Linear sweep voltammograms of NCNTs after treatment in 10 M KOH at 80 °C for 5 h (in O_2-saturated 0.1 M KOH at a scan rate of 5 mV s^{-1} and a rotation rate of 100 rpm).

potential of NCNT-growth at 0.913 V was about 24 mV more positive than that for NCNT-NH_3 and NCNT-aniline (Table 1). NCNT-growth also showed higher reduction currents than NCNT-aniline and NCNT-NH_3. For example, at 0.2 V the reduction current density of NCNT-growth increased by 0.29 mA cm^{-2} after the alkaline treatment, whereas those of NCNT-aniline and NCNT-NH_3 decreased by 0.32 and 0.16 mA cm^{-2}, respectively. Overall, the ORR activity in 0.1 M KOH decreases in the sequence NCNT-growth > NCNT-aniline > NCNT-NH_3 after alkaline treatment as determined by their onset potentials (Figure 2), in contrast to the order NCNT-NH_3 > NCNT-aniline > NCNT-growth before the treatment (Figure 1a). These differences underline the changes in the active sites due to the alkaline treatment. This is particularly reflected in

dx.doi.org/10.1021/jp4059438 | J. Phys. Chem. C 2013, 117, 24283−24291

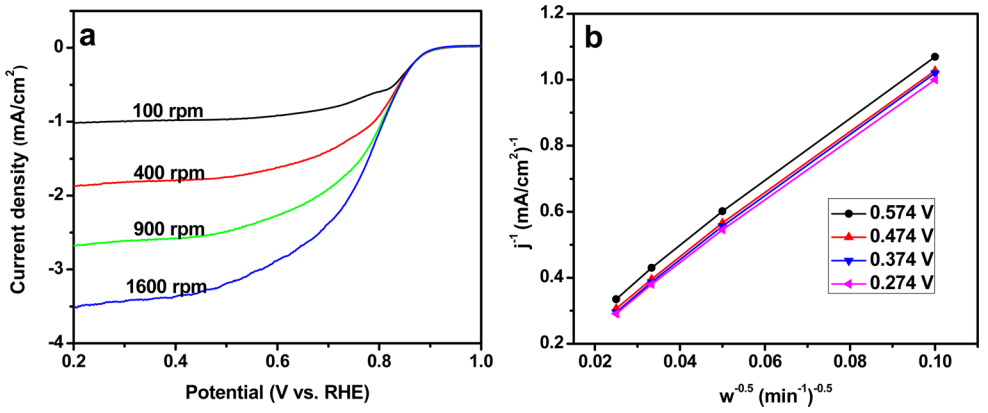

Figure 3. (a) RDE polarization curves recorded for NCNT-NH_3 in O_2-saturated 0.1 M KOH at a scan rate of 5 mV s^{-1} and different rotation rates. (b) Koutecky–Levich plots of data extracted from (a).

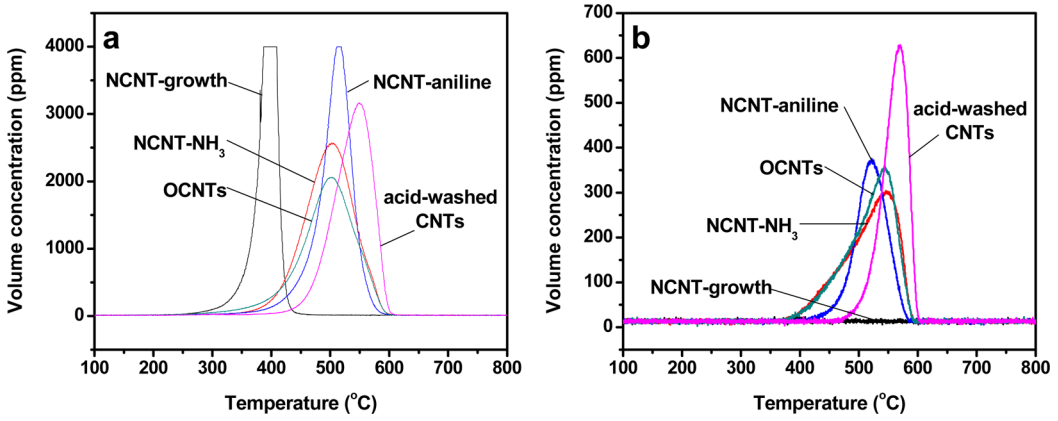

Figure 4. (a) CO_2 and (b) CO profiles of acid-washed CNTs, OCNTs, and the three types of NCNTs. The measurements were carried out by heating 5.0 mg of sample from room temperature to 800 °C at a heating rate of 1 K min^{-1} in 5 vol % O_2 in helium.

the sudden change in the slope of the NCNT-aniline sample at 0.794 V, which was not observed prior to the treatment.

The RDE results were used to analyze the reaction mechanism and kinetics. As a typical example, RDE polarization curves of NCNT-NH_3 after alkaline treatment at different rotation rates in 0.1 M KOH are shown in Figure 3a. As expected, the current density increases with increasing rotation rate from 100 to 1600 rpm. The corresponding Koutecky–Levich plots over the potential range from 0.574 to 0.274 V are shown in Figure 3b. In particular, the number of transferred electrons does not change in the given potential range, and the reaction is first order with respect to the oxygen concentration. The polarization curves and Koutecky–Levich plots of the other samples showed similar features in 0.1 and 1.0 M KOH solutions (not shown).

The electron transfer number (n) for the different NCNTs were calculated from the slope of the Koutecky–Levich plots following the procedure reported in the literature.[34] The following parameters were used for the calculations: for an oxygen-saturated 0.1 M KOH solution, the oxygen concentration $C_0^* = 1.20 \times 10^{-3}$ mol L^{-1}, the oxygen diffusion coefficient $D_0 = 1.90 \times 10^{-5}$ cm^2 s^{-1}, and the viscosity of the electrolyte $\nu = 1.00 \times 10^{-2}$ cm^2 s^{-1};[38] for 1.0 M KOH, $C_0^* = 0.84 \times 10^{-3}$ mol L^{-1}, $D_0 = 1.43 \times 10^{-5}$ cm^2 s^{-1}, and $\nu = 1.13 \times 10^{-2}$ cm^2 s^{-1}.[39] Table 1 shows the electron transfer numbers at 0.374 V in 0.1 and 1.0 M KOH electrolytes. In 0.1 M KOH, the oxygen reduction occurred through a mixed two-electron/four-electron pathway. The electron transfer number was determined to be 2.9 for NCNT-growth and NCNT-NH_3, whereas n was found to be 3.4 for NCNT-aniline, indicating a higher selectivity for the four-electron transfer reduction of oxygen. The electron transfer numbers of all three samples, that is, 3.2 for NCNT-growth, 3.3 for NCNT-NH_3, and 3.8 for NCNT-aniline, were higher in 1.0 M KOH than in 0.1 M KOH. After alkaline treatment, n was 4.0 for NCNT-growth in 0.1 M KOH, suggesting a direct four-electron pathway, but n for NCNT-NH_3 and n for NCNT-aniline were less than 3. These results confirmed the changes in the active sites due to the treatment in 10 M KOH.

3.2. Thermal Stability. The degree of structural order is a key factor which affects the stability of carbon materials. The corrosion of carbon materials is known to occur more rapidly at defect sites.[26] Correspondingly, the thermal stability can be used to characterize the structural order of carbon materials. The NCNT catalysts were studied by temperature-programmed oxidation (TPO) in the gas phase and compared with acid-washed CNTs and oxygen-functionalized CNTs (OCNTs). NCNT-growth showed a considerably lower oxidation resistance than all the other samples as indicated by the CO_2 peak at much lower temperatures (Figure 4a), which can be attributed to surface defects and structural disorders due to the presence of N in the carbon lattice.[40,41] In contrast, CNTs purified by washing in diluted acid showed the highest thermal resistance of all the samples. Both oxygen functionalization (OCNTs) and the incorporation of nitrogen (NCNT-NH_3 and NCNT-aniline) led to a decrease of the oxidation resistance as

dx.doi.org/10.1021/jp4059438 | J. Phys. Chem. C 2013, 117, 24283–24291

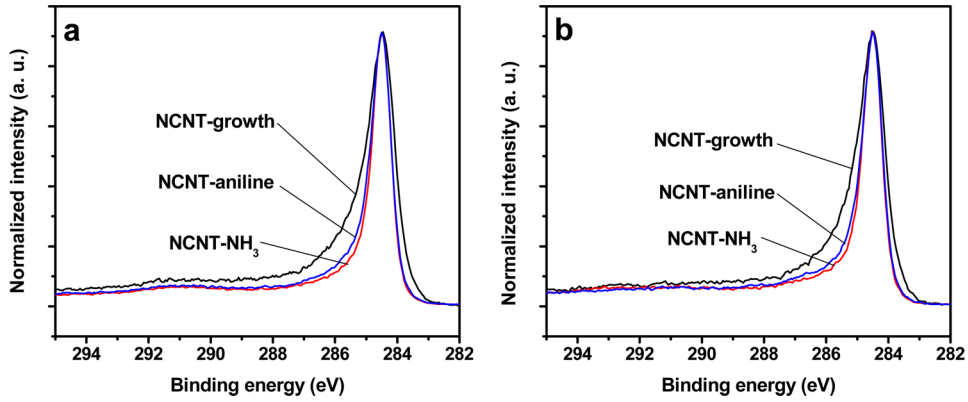

Figure 5. XP C 1s spectra of the NCNTs (a) before and (b) after alkaline treatment in 10 M KOH at 80 °C for 5 h. The spectra were normalized to the corresponding C 1s peaks.

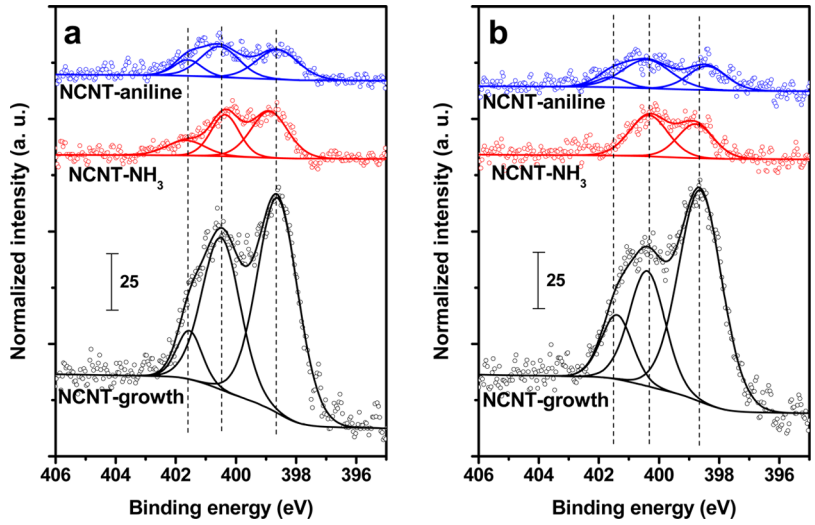

Figure 6. XP N 1s spectra of NCNTs (a) before and (b) after alkaline treatment in 10 M KOH at 80 °C for 5 h. The spectra were normalized to the corresponding C 1s peaks.

indicated by CO_2 peaks at lower temperatures. The CO_2 peak position of NCNT-NH_3 is rather close to that of OCNTs at around 500 °C, but the initial oxidation temperature of NCNT-NH_3 was 65 °C higher than that of OCNTs, which is presumably related to the decomposition of oxygen-containing groups on OCNTs. Hence, the bulk structure of OCNTs is similar to that of NCNT-NH_3 with differences only on the surface. Different from the surface effects introduced by the NH_3 treatment, the CO_2 peaks shifted to a higher temperature for NCNT-aniline, which can be related to the presence of a nitrogen-doped carbon coating or amorphous carbon on the surface.[36]

The CO profiles of the samples are shown in Figure 4b. The release of CO occurred at higher temperatures than that of CO_2 for all samples. The asymmetry of the peaks can be attributed to the decomposition of surface oxygen groups. It is remarkable that the NCNT-growth sample showed only a negligible CO peak. These results indicate that the thermal stability of CNTs is related to surface and bulk defects as well as to surface functional groups involving heteroatoms. It is reasonable to assume that these factors can also affect the electrochemical long-term stability. Although the NCNT-growth sample showed very promising electrocatalytic activity, it may have substantial stability problems during long-term operation.

3.3. XPS Studies. High-resolution XPS measurements were performed with the NCNT samples before and after alkaline treatment. Carbon, oxygen, and nitrogen were detected in the survey spectra, but no metallic species were detected. The region spectra were normalized to the intensity of the C 1s peak of graphitic carbon at 284.5 eV. The C 1s peak of NCNT-growth was much broader than those of NCNT-NH_3 and NCNT-aniline (Figure 5a), which is due to the higher nitrogen doping level in NCNT-growth.[42] NCNT-aniline showed a more pronounced shoulder between 285 and 286 eV than NCNT-NH_3, which can be related to organic carbon species that were not fully carbonized during the aniline treatment. The C 1s spectra did not show significant changes after the treatment in 10 M KOH (Figure 5b) because of the substantial inelastic mean free path in carbon materials.

The deconvoluted XP N 1s spectra of the NCNTs are shown in Figure 6. NCNT-growth showed a clearly higher intensity in the N 1s region than NCNT-NH_3 and NCNT-aniline, indicating higher nitrogen content. The N 1s spectra of the NCNT samples can be deconvoluted into three contributions at 398.5 eV (N1), 400.5 eV (N2), and 401.5 eV (N3) corresponding to pyridinic, pyrrolic, and quaternary-type nitrogen groups, respectively.[24,43,44] After alkaline treatment, a clear increase of the pyridinic-N concentration was observed in NCNT-growth as indicated by the strong peak at 398.5 eV,

dx.doi.org/10.1021/jp4059438 | J. Phys. Chem. C 2013, 117, 24283−24291

whereas the concentration of pyridinic-N decreased in NCNT-NH_3 and NCNT-aniline. Only two peaks can be fitted for the sample NCNT-NH_3 after the alkaline treatment, indicating the absence of quaternary N (Figure 6b).

Quantitative analysis of the N 1s spectra was carried out to determine the N/C ratio and the relative concentrations of different nitrogen groups in the NCNTs (Table 2). NCNT-growth showed a significantly higher N/C ratio than NCNT-NH_3 and NCNT-aniline. In comparison to the ORR results in Figure 1a, it can be seen that the ORR activity is not directly correlated to the total nitrogen amount, which is in good agreement with our earlier studies.[34] The treatment in 10 M KOH led to a slight decrease of the N/C ratio for all three NCNT samples (Table 2). Moreover, the relative concentrations of N groups changed differently after the alkaline treatment. For NCNT-growth, the concentrations of pyridinic- and quaternary-N increased, while that of pyrrolic-N decreased, whereas NCNT-NH_3 and NCNT-aniline exhibited the opposite trend.

Table 2. N/C Ratios and Relative Concentrations of Different Nitrogen Groups Obtained by Deconvolution of the XP N 1s Spectra

	before alkaline treatment				after alkaline treatment[a]			
sample	N/C (10^{-2})	N1[b] (%)	N2 (%)	N3 (%)	N/C (10^{-2})	N1 (%)	N2 (%)	N3 (%)
NCNT-growth	4.8	55	37	8	4.8	60	27	13
NCNT-NH_3	1.6	49	34	17	1.3	44	56	–
NCNT-aniline	1.2	43	41	16	1.1	35	53	12

[a]The alkaline treatment was performed in 10 M KOH at 80 °C for 5 h. [b]N1, pyridinic-N; N2, pyrrolic-N; N3, quaternary-N.

The concentration of quaternary-N was considered to be one of the main factors influencing ORR catalysis.[29,31,38] Pyridinic-N was also assumed to be responsible for ORR catalysis, which can be related to the conjugation effect of the nitrogen lone pair electrons and the graphene π system.[27,28] By carefully comparing the ORR activity in Figures 1 and 2 and the relative concentrations of different N groups in Table 2, it can be concluded that high concentrations of pyridinic-N and quaternary-N are beneficial for the ORR catalysis, whereas pyrrolic-N shows mainly a negative effect.

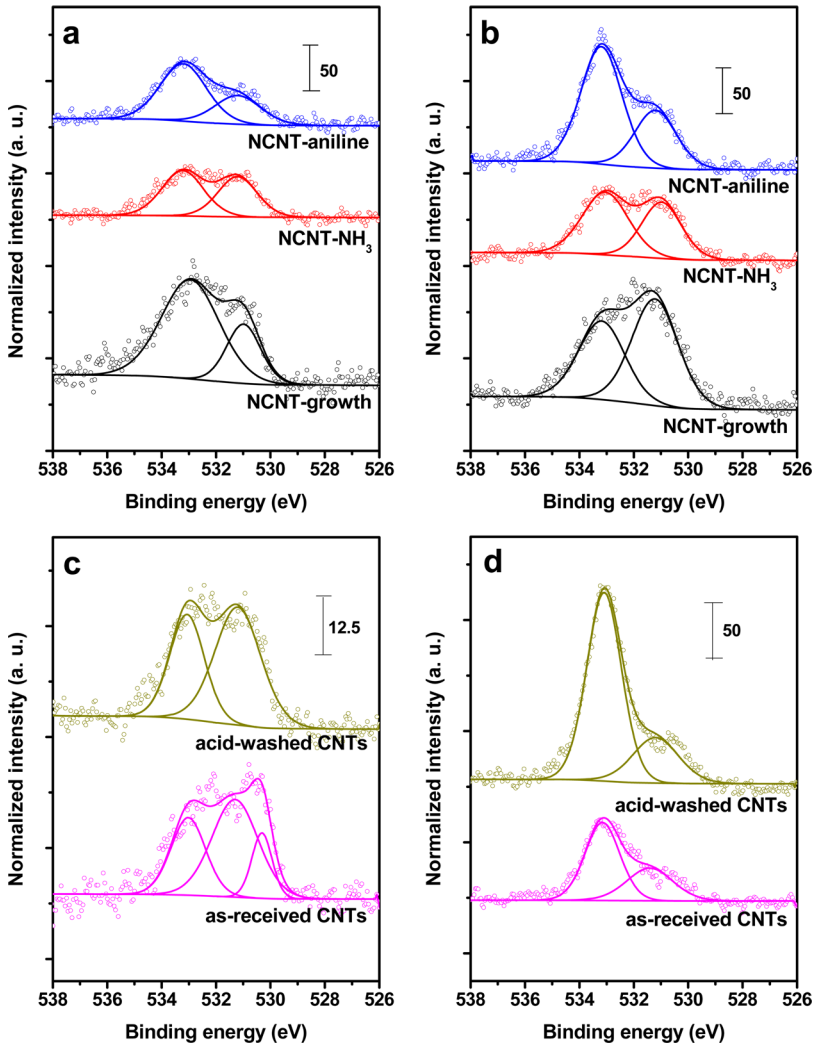

Figure 7. XP O 1s spectra of samples before and after alkaline treatment in 10 M KOH at 80 °C for 5 h. (a) NCNTs before treatment, (b) NCNTs after treatment, (c) CNTs before treatment, and (d) CNTs after treatment. The spectra were normalized to the corresponding C 1s peaks.

dx.doi.org/10.1021/jp4059438 | J. Phys. Chem. C 2013, 117, 24283−24291

The corrosion of carbon is an oxidation process involving the formation of oxygen groups on the carbon surface. Hence, the XP O 1s spectra of the NCNT samples before and after alkaline treatment were measured and are shown in Figure 7a, b. Mainly two contributions were detected in the O 1s region corresponding to an oxygen−carbon double bond (C═O) at 531.2 eV and oxygen−carbon single bond (C−O) at 533.1 eV.[36] NCNT-growth had a higher oxygen concentration than NCNT-NH_3 and NCNT-aniline before the treatment in 10 M KOH (Figure 7a). The alkaline treatment led to an increase of the oxygen concentration in all samples (Figure 7b). In particular, the intensity of the C═O groups in the NCNT-growth sample was significantly increased by this treatment.

For comparison, as-received CNTs and CNTs purified by acid washing were evaluated before and after alkaline treatment (Figure 7c, d). Both samples show a strong increase in the oxygen concentration caused by the treatment. In addition to the C═O and C−O peaks, a contribution signal at about 530.3 eV was observed in the O 1s spectrum of as-received CNTs, which can be assigned to metal oxides used as catalysts for CNT growth. These metal oxides were nearly entirely removed by alkaline treatment as indicated by the O 1s spectra (Figure 7d).

Quantitative analysis of the XP O 1s spectra is summarized in Table 3. The total oxygen concentration increased in all samples due to alkaline treatment. The strongest increase from 1.5 to 5.3% was recorded in the acid-washed CNTs, indicating that the residual catalysts in as-received CNTs promote the decomposition of oxygen groups.[45] Hence, a much lower increase in total oxygen concentration was observed for the as-received CNTs (Table 3). It is assumed that the formation of stable surface oxygen species mainly occurs on carbon sites, whereas the oxygen directly associated with nitrogen such as $-NO_x$ species decomposes during drying under mild conditions. The absence of $-NO_x$ was confirmed by XPS studies (Figure 6 and Table 2). A strong increase in the total oxygen concentration was detected for NCNT-aniline and NCNT-NH_3, whereas only a slight increase was recorded for NCNT-growth (Table 3). This difference can be related to the total nitrogen amount on the surface. The surface of NCNT-growth is largely occupied by nitrogen species (N/C = 4.8×10^{-2}), and free active carbon sites are limited. In contrast, much higher amounts of free carbon sites are present on NCNT-aniline (N/C = 1.6×10^{-2}) and NCNT-NH_3 (N/C = 1.2×10^{-2}), which provides the possibility for anchoring additional oxygen species. It is known from density functional theory calculations that the presence of nitrogen can enhance the dissociative adsorption of O_2 at carbon sites.[31] Hence, the formation of oxygen species seems to be promoted by nitrogen species, provided that free carbon sites are available.

Table 3. O/C Ratios and Relative Concentrations of Oxygen Groups Obtained by Deconvolution of the XP O 1s Spectra

	before alkaline treatment[a]			after alkaline treatment[a]		
sample	O/C (10^{-2})	C═O (%)	C−O (%)	O/C (10^{-2})	C═O (%)	C−O (%)
NCNT-growth	4.0	26	74	4.6	58	42
NCNT-NH_3	2.7	46	54	4.1	44	56
NCNT-aniline	2.8	33	67	5.3	33	67
acid-washed CNTs	1.5	60	40	5.3	24	76
as-received CNTs	1.4	53	32	2.8	36	64

[a]The alkaline treatment was performed in 10 M KOH at 80 °C for 5 h.

The relative changes in C═O and C−O as determined by XPS are shown in Table 3. For the two samples without nitrogen, a strong increase in C−O was observed after alkaline treatment accompanied by a relative decrease of C═O species. This observation indicates that the formation of oxygen groups under strong alkaline conditions is related to the adsorption of hydroxyl groups at the exposed CNT surfaces. The relative concentrations of C═O and C−O remain largely unchanged for NCNT-aniline and NCNT-NH_3. In contrast, a strong increase in C═O concentration was recorded for NCNT-growth after the alkaline treatment.

Scheme 1 shows the oxygen and nitrogen species that are presumably present on the exposed carbon surfaces. The incorporation of oxygen species in NCNTs by alkaline treatment in 10 M KOH at 80 °C can occur following three different pathways. (1) In the case of large nitrogen-free areas, oxygen species attack carbon at defect sites, preferably forming C−OH. (2) Nitrogen activates neighboring carbon atoms, which then anchor oxygen species, forming C−OH or C═O. (3) When the surface has been largely occupied by nitrogen and oxygen species as in NCNT-growth, nitrogen species may decompose upon attack by OH^-, forming preferably C═O. However, the nitrogen species appeared to be very stable at the used alkaline conditions, and hence decomposition of nitrogen occurred only to a small extent. Generally, it is assumed that the species with oxygen and nitrogen on adjacent sites such as pyridone and lactam are not high-temperature-stable species. These species can be formed in the liquid phase upon alkaline treatment, but decompose at elevated temperatures in the gas phase.

Scheme 1. Surface Groups of Three Types of NCNTs after Alkaline Treatment

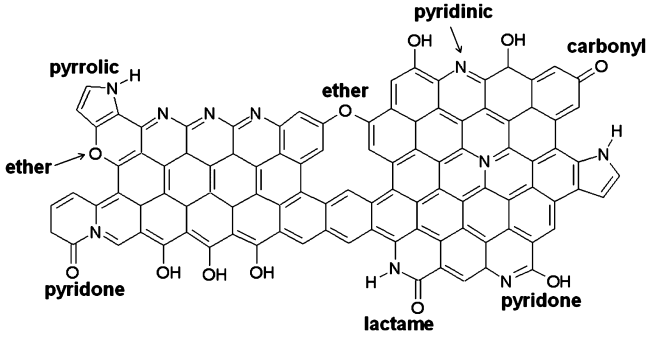

4. CONCLUSIONS

Three types of NCNTs synthesized by catalytic growth or by posttreatment with NH_3 and aniline were treated in 10 M KOH at 80 °C for 5 h and tested as electrocatalysts in the ORR. Before treatment, the NCNT-NH_3 sample showed the highest ORR activity. After treatment, NCNT-growth showed enhanced catalytic activity in contrast to the decreased performances of NCNT-NH_3 and NCNT-aniline. NCNT-growth showed the lowest thermal stability against oxidation in the gas phase due to the highest degree of structural disorder. The XPS analysis showed that the ORR activity was not correlated to the total nitrogen amount, but was correlated to the concentrations of pyridinic and quaternary nitrogen groups.

dx.doi.org/10.1021/jp4059438 | J. Phys. Chem. C 2013, 117, 24283−24291

A significant increase in oxygen concentration was observed for all samples after treatment in 10 M KOH. In the absence of nitrogen, a strong increase of C−O was observed. In contrast, the sample NCNT-growth showed a strong increase in C═O, indicating that nitrogen in NCNTs influences surface oxidation and formation of oxygen groups on carbon.

AUTHOR INFORMATION

Corresponding Author

*E-mail: wei.xia@techem.rub.de. Fax: (+49) 234 32 14115.

Notes

The authors declare no competing financial interest.

ACKNOWLEDGMENTS

The authors thank Martin Muhler for stimulating discussion and the Federal Ministry of Education and Research (BMBF) for financial support (Inno.CNT Project CarboElch, Grant 03X0207C). The authors are grateful to all partners in the project for the fruitful cooperation. A.Z. thanks the China Scholarship Council for a research grant.

REFERENCES

(1) Spendelow, J. S.; Wieckowski, A. Electrocatalysis of Oxygen Reduction and Small Alcohol Oxidation in Alkaline Media. *Phys. Chem. Chem. Phys.* **2007**, *9*, 2654−2675.

(2) Guo, J.; Hsu, A.; Chu, D.; Chen, R. Improving Oxygen Reduction Reaction Activities on Carbon-Supported Ag Nanoparticles in Alkaline Solutions. *J. Phys. Chem. C* **2010**, *114*, 4324−4330.

(3) Lee, J.-S.; Kim, S. T.; Cao, R.; Choi, N.-S.; Liu, M.; Lee, K. T.; Cho, J. Metal−Air Batteries with High Energy Density: Li−Air Versus Zn−Air. *Adv. Energy Mater.* **2011**, *1*, 34−50.

(4) Lipp, L.; Gottesfeld, S.; Chlistunoff, J. Peroxide Formation in a Zero-Gap Chlor-Alkali Cell with an Oxygen-Depolarized Cathode. *J. Appl. Electrochem.* **2005**, *35*, 1015−1024.

(5) Yang, Z.; Zhou, X.; Nie, H.; Yao, Z.; Huang, S. Facile Construction of Manganese Oxide Doped Carbon Nanotube Catalysts with High Activity for Oxygen Reduction Reaction and Investigations into the Origin of Their Activity Enhancement. *ACS Appl. Mater. Interfaces* **2011**, *3*, 2601−2606.

(6) Jin, C.; Nagaiah, T. C.; Xia, W.; Bron, M.; Schuhmann, W.; Muhler, M. Polythiophene-Assisted Vapor Phase Synthesis of Carbon Nanotube-Supported Rhodium Sulfide as Oxygen Reduction Catalyst for HCl Electrolysis. *ChemSusChem* **2011**, *4*, 927−930.

(7) Lu, Y.; Chen, W. Size Effect of Silver Nanoclusters on Their Catalytic Activity for Oxygen Electro-Reduction. *J. Power Sources* **2012**, *197*, 107−110.

(8) Wiberg, G. K. H.; Mayrhofer, K. J. J.; Arenz, M. Investigation of the Oxygen Reduction Activity on Silver—A Rotating Disc Electrode Study. *Fuel Cells* **2010**, *10*, 575−581.

(9) Sudoh, M.; Arai, K.; Izawa, Y.; Suzuki, T.; Uno, M.; Tanaka, M.; Hirao, K.; Nishiki, Y. Evaluation of Ag-Based Gas-Diffusion Electrode for Two-Compartment Cell Used in Novel Chlor-Alkali Membrane Process. *Electrochim. Acta* **2011**, *56*, 10575−10581.

(10) Chen, Z.; Yu, A.; Ahmed, R.; Wang, H.; Li, H.; Chen, Z. Manganese Dioxide Nanotube and Nitrogen-Doped Carbon Nanotube Based Composite Bifunctional Catalyst for Rechargeable Zinc-Air Battery. *Electrochim. Acta* **2012**, *69*, 295−300.

(11) Gorlin, Y.; Jaramillo, T. F. A Bifunctional Nonprecious Metal Catalyst for Oxygen Reduction and Water Oxidation. *J. Am. Chem. Soc.* **2010**, *132*, 13612−13614.

(12) Lefevre, M.; Proietti, E.; Jaouen, F.; Dodelet, J.-P. Iron-Based Catalysts with Improved Oxygen Reduction Activity in Polymer Electrolyte Fuel Cells. *Science* **2009**, *324*, 71−74.

(13) Tang, Y.; Allen, B. L.; Kauffman, D. R.; Star, A. Electrocatalytic Activity of Nitrogen-Doped Carbon Nanotube Cups. *J. Am. Chem. Soc.* **2009**, *131*, 13200−13201.

(14) Rao, C. V.; Ishikawa, Y. Activity, Selectivity, and Anion-Exchange Membrane Fuel Cell Performance of Virtually Metal-Free Nitrogen-Doped Carbon Nanotube Electrodes for Oxygen Reduction Reaction. *J. Phys. Chem. C* **2012**, *116*, 4340−4346.

(15) Higgins, D.; Chen, Z.; Chen, Z. Nitrogen Doped Carbon Nanotubes Synthesized from Aliphatic Diamines for Oxygen Reduction Reaction. *Electrochim. Acta* **2011**, *56*, 1570−1575.

(16) Wang, Z.; Jia, R.; Zheng, J.; Zhao, J.; Li, L.; Song, J.; Zhu, Z. Nitrogen-Promoted Self-Assembly of N-Doped Carbon Nanotubes and Their Intrinsic Catalysis for Oxygen Reduction in Fuel Cells. *ACS Nano* **2011**, *5*, 1677−1684.

(17) Ma, Y.; Sun, L.; Huang, W.; Zhang, L.; Zhao, J.; Fan, Q.; Huang, W. Three-Dimensional Nitrogen-Doped Carbon Nanotubes/Graphene Structure Used as a Metal-Free Electrocatalyst for the Oxygen Reduction Reaction. *J. Phys. Chem. C* **2011**, *115*, 24592−24597.

(18) Chen, S.; Bi, J.; Zhao, Y.; Yang, L.; Zhang, C.; Ma, Y.; Wu, Q.; Wang, X.; Hu, Z. Nitrogen-Doped Carbon Nanocages as Efficient Metal-Free Electrocatalysts for Oxygen Reduction Reaction. *Adv. Mater.* **2012**, *24*, 5593−5597.

(19) Gong, K.; Du, F.; Xia, Z.; Durstock, M.; Dai, L. Nitrogen-Doped Carbon Nanotube Arrays with High Electrocatalytic Activity for Oxygen Reduction. *Science* **2009**, *323*, 760−764.

(20) Yu, D.; Zhang, Q.; Dai, L. Highly Efficient Metal-Free Growth of Nitrogen-Doped Single-Walled Carbon Nanotubes on Plasma-Etched Substrates for Oxygen Reduction. *J. Am. Chem. Soc.* **2010**, *132*, 15127−15129.

(21) Zhao, Y.; Yang, L.; Chen, S.; Wang, X.; Ma, Y.; Wu, Q.; Jiang, Y.; Qian, W.; Hu, Z. Can Boron and Nitrogen Co-Doping Improve Oxygen Reduction Reaction Activity of Carbon Nanotubes? *J. Am. Chem. Soc.* **2013**, *135*, 1201−1204.

(22) Zheng, Y.; Jiao, Y.; Ge, L.; Jaroniec, M.; Qiao, S. Z. Two-Step Boron and Nitrogen Doping in Graphene for Enhanced Synergistic Catalysis. *Angew. Chem., Int. Ed.* **2013**, *52*, 3110−3116.

(23) Kundu, S.; Xia, W.; Busser, W.; Becker, M.; Schmidt, D. A.; Havenith, M.; Muhler, M. The Formation of Nitrogen-Containing Functional Groups on Carbon Nanotube Surfaces: A Quantitative XPS and TPD Study. *Phys. Chem. Chem. Phys.* **2010**, *12*, 4351−4359.

(24) Mao, L.; Zhang, D.; Sotomura, T.; Nakatsu, K.; Koshiba, N.; Ohsaka, T. Mechanistic Study of the Reduction of Oxygen in Air Electrode with Manganese Oxides as Electrocatalysts. *Electrochim. Acta* **2003**, *48*, 1015−1021.

(25) Wiggins-Camacho, J. D.; Stevenson, K. J. Effect of Nitrogen Concentration on Capacitance, Density of States, Electronic Conductivity, and Morphology of N-Doped Carbon Nanotube Electrodes. *J. Phys. Chem. C* **2009**, *113*, 19082−19090.

(26) Li, C.; Zhao, A.; Xia, W.; Liang, C.; Muhler, M. Quantitative Studies on the Oxygen and Nitrogen Functionalization of Carbon Nanotubes Performed in the Gas Phase. *J. Phys. Chem. C* **2012**, *116*, 20930−20936.

(27) Sidik, R. A.; Anderson, A. B.; Subramanian, N. P.; Kumaraguru, S. P.; Popov, B. N. O2 Reduction on Graphite and Nitrogen-Doped Graphite: Experiment and Theory. *J. Phys. Chem. B* **2006**, *110*, 1787−1793.

(28) Kurak, K. A.; Anderson, A. B. Nitrogen-Treated Graphite and Oxygen Electroreduction on Pyridinic Edge Sites. *J. Phys. Chem. C* **2009**, *113*, 6730−6734.

(29) Nagaiah, T. C.; Kundu, S.; Bron, M.; Muhler, M.; Schuhmann, W. Nitrogen-Doped Carbon Nanotubes as a Cathode Catalyst for the Oxygen Reduction Reaction in Alkaline Medium. *Electrochem. Commun.* **2010**, *12*, 338−341.

(30) Sharifi, T.; Hu, G.; Jia, X.; Wagberg, T. Formation of Active Sites for Oxygen Reduction Reactions by Transformation of Nitrogen Functionalities in Nitrogen-Doped Carbon Nanotubes. *ACS Nano* **2012**, *6*, 8904−8912.

(31) Ikeda, T.; Boero, M.; Huang, S.-F.; Terakura, K.; Oshima, M.; Ozaki, J. Carbon Alloy Catalysts: Active Sites for Oxygen Reduction Reaction. *J. Phys. Chem. C* **2008**, *112*, 14706−14709.

(32) Artyushkova, K.; Pylypenko, S.; Olson, T. S.; Fulghum, J. E.; Atanassov, P. Predictive Modeling of Electrocatalyst Structure Based

on Structure-to-Property Correlations of X-Ray Photoelectron Spectroscopic and Electrochemical Measurements. *Langmuir* **2008**, *24*, 9082−9088.
(33) Wiggins-Camacho, J. D.; Stevenson, K. J. Mechanistic Discussion of the Oxygen Reduction Reaction at Nitrogen-Doped Carbon Nanotubes. *J. Phys. Chem. C* **2011**, *115*, 20002−20010.
(34) Zhao, A.; Masa, J.; Muhler, M.; Schuhmann, W.; Xia, W. N-Doped Carbon Synthesized from N-Containing Polymers as Metal-Free Catalysts for the Oxygen Reduction under Alkaline Conditions. *Electrochim. Acta* **2013**, *98*, 139−145.
(35) Kundu, S.; Nagaiah, T. C.; Xia, W.; Wang, Y.; Van Dommele, S.; Bitter, J. H.; Santa, M.; Grundmeier, G.; Bron, M.; Schuhmann, W.; Muhler, M. Electrocatalytic Activity and Stability of Nitrogen-Containing Carbon Nanotubes in the Oxygen Reduction Reaction. *J. Phys. Chem. C* **2009**, *113*, 14302−14310.
(36) Jin, C.; Nagaiah, T. C.; Xia, W.; Spliethoff, B.; Wang, S.; Bron, M.; Schuhmann, W.; Muhler, M. Metal-Free and Electrocatalytically Active Nitrogen-Doped Carbon Nanotubes Synthesized by Coating with Polyaniline. *Nanoscale* **2010**, *2*, 981−987.
(37) Xia, W.; Jin, C.; Kundu, S.; Muhler, M. A Highly Efficient Gas-Phase Route for the Oxygen Functionalization of Carbon Nanotubes Based on Nitric Acid Vapor. *Carbon* **2009**, *47*, 919−922.
(38) Xia, W.; Masa, J.; Bron, M.; Schuhmann, W.; Muhler, M. Highly Active Metal-Free Nitrogen-Containing Carbon Catalysts for Oxygen Reduction Synthesized by Thermal Treatment of Polypyridine-Carbon Black Mixtures. *Electrochem. Commun.* **2011**, *13*, 593−596.
(39) Roche, I.; Chainet, E.; Chatenet, M.; Vondrak, J. Carbon-Supported Manganese Oxide Nanoparticles as Electrocatalysts for the Oxygen Reduction Reaction (ORR) in Alkaline Medium: Physical Characterizations and ORR Mechanism. *J. Phys. Chem. C* **2007**, *111*, 1434−1443.
(40) Nxumalo, E. N.; Coville, N. J. Nitrogen Doped Carbon Nanotubes from Organometallic Compounds: A Review. *Materials* **2010**, *3*, 2141−2171.
(41) Kurt, R.; Karim, A. Influence of Nitrogen on the Growth Mechanism of Decorated C:N Nanotubes. *ChemPhysChem* **2001**, *2*, 388−392.
(42) Maldonado, S.; Morin, S.; Stevenson, K. J. Structure, Composition, and Chemical Reactivity of Carbon Nanotubes by Selective Nitrogen Doping. *Carbon* **2006**, *44*, 1429−1437.
(43) Casanovas, J.; Ricart, J. M.; Rubio, J.; Illas, F.; Jimenez-Mateos, J. M. Origin of the Large N 1s Binding Energy in X-Ray Photoelectron Spectra of Calcined Carbonaceous Materials. *J. Am. Chem. Soc.* **1996**, *118*, 8071−8076.
(44) Yang, Z.; Xia, Y.; Mokaya, R. Aligned N-Doped Carbon Nanotube Bundles Prepared via CVD Using Zeolite Substrates. *Chem. Mater.* **2005**, *17*, 4502−4508.
(45) Hamdani, M.; Singh, R. N.; Chartier, P. Co3O4 and Co- Based Spinel Oxides Bifunctional Oxygen Electrodes. *Int. J. Electrochem. Sci.* **2010**, *5*, 556−577.